NASA TECHNICAL NOTE

NASA TN D-5122

C. 1

NASA TN D-5122

INVESTIGATION OF A PLASMA ACCELERATOR WITH MAGNETIC FIELD ARRANGED TO PRODUCE A DIVERGENT-NOZZLE EFFECT

by Joseph D. Brooks and William D. Beasley

Langley Research Center
Langley Station, Hampton, Va.

NATIONAL AERONAUTICS AND SPACE ADMINISTRATION • WASHINGTON, D. C. • APRIL 1969

INVESTIGATION OF A PLASMA ACCELERATOR WITH MAGNETIC FIELD ARRANGED TO PRODUCE A DIVERGENT-NOZZLE EFFECT

By Joseph D. Brooks and William D. Beasley

Langley Research Center
Langley Station, Hampton, Va.

NATIONAL AERONAUTICS AND SPACE ADMINISTRATION

For sale by the Clearinghouse for Federal Scientific and Technical Information
Springfield, Virginia 22151 – CFSTI price $3.00

INVESTIGATION OF A PLASMA ACCELERATOR WITH MAGNETIC FIELD ARRANGED TO PRODUCE A DIVERGENT-NOZZLE EFFECT

By Joseph D. Brooks and William D. Beasley
Langley Research Center

SUMMARY

The results of an experimental investigation of a plasma accelerator are presented at static pressures from 0.765 mm Hg to 2.60 mm Hg. The continuous-flow device uses a dc arc to provide the plasma and a dc magnetic field that is shaped to provide both the constriction of the plasma and the pressure gradient that produces the flow.

Pressure measurements showed that within a certain range of parameters a supersonic flow was obtained. With an increase in magnetic field strength and arc current the Mach number increased, and with an increase in pressure the Mach number decreased. The maximum pressure ratio obtained was 40.

INTRODUCTION

The possibility of using a magnetic field to constrict a plasma flow in such a manner as to produce an effect similar to that of a physical nozzle has been the subject of several investigations. (See, for instance, refs. 1 and 2.) Such a device would have the advantage of providing a high-temperature flow with neither loss of material from the walls (ref. 3) nor significant loss of energy to the walls. On the other hand, the conventional "magnetic nozzle" concept with the plasma generator separated from the magnetic nozzle incurs the serious problem of losses of energy, ionization, and wall material in the region between the plasma-producing discharge and the magnetic field.

The system described in this paper represents an attempt to overcome this problem by combining the expansion region of a magnetic-nozzle field configuration with plasma production and acceleration means. The feasibility of such a system was suggested by the experiments reported in reference 4, which indicated that a magnetic field parallel to the axis of an arc could maintain a pressure differential of 75 mm Hg between the pressure in the arc and the ambient pressure in the chamber. The present system was designed to supply the nozzle pressure ratio, not by the superimposed longitudinal pressure gradient of a physical nozzle, but by compression of the arc plasma by the magnetic field. The

resulting design bears a resemblance to plasma accelerators having axisymmetric geometry and termed variously "Hall current accelerators," "magnetoplasmadynamic arcs," and so forth, in the literature (ref. 4).

However, there is a significant design difference. Whereas most of the axisymmetric geometry devices studied heretofore have endeavored to produce strong magnetohydrodynamic acceleration effects by incorporating as a design feature a relative positioning of electrodes and magnetic field coil that will force the current to flow through the gas across the field lines, the present system is designed to permit a free-current flow through the gas along the field lines.

SYMBOLS

B	magnetic flux density, gauss
B_0	magnetic flux density at geometrical center of coil, gauss
I	current in arc, amperes
j	current density, amperes per square centimeter
L	half-length of coil, 2.38 centimeters
p	static pressure measured at wall, millimeters of mercury
p_t	pitot pressure, measured at the center line of the flow, millimeters of mercury
r,z	radial and longitudinal distances from geometrical center of coil, centimeters

Subscripts:

r,θ,z	radial, azimuthal, and longitudinal components, respectively

GENERAL DESIGN CONSIDERATIONS

As noted in the introduction, many magnetohydrodynamic devices employing an axisymmetric electrode-field arrangement have been investigated (ref. 4) under the designation MPD arc or coaxial Hall current accelerator.

However, the design of the system described herein was inspired by the work reported in reference 5. There, it was demonstrated that when a helium arc was maintained in a nearly homogeneous magnetic field of about 23 kilogauss, the pressure within the arc was approximately 80 mm Hg, while the ambient chamber pressure was only 6 mm Hg. In view of this result, the present investigation was based on the following considerations: If a strong magnetic field were applied near one end (the cathode end) of the arc but decreased sharply along the length of the arc, then there would be a longitudinal easing of the magnetic constriction and consequently a longitudinal gas-pressure gradient would be produced in the arc. This pressure gradient would result in a plasma flow expanding out along the diverging magnetic field lines.

As the charged particles were ejected from the arc in this manner, the plasma would be replenished by the diffusion of neutral particles into the arc, where they would become ionized and "trapped" in the magnetic field. Thus, the mechanism would be somewhat similar to that occurring in the cathode jet resulting from the self-magnetic field constriction of an arc characterized by a high current density in the region of a cathode spot (ref. 6 and p. 38 of ref. 7), except that in this case the magnetic field would be imposed on the arc plasma and applied longitudinally rather than circumferentially.

The possibility of a kind of supersonic nozzle mechanism exists as a result of the expansion of the arc plasma along the strongly diverging field lines, together with the pressure differential produced by the magnetic constriction. It is of interest to consider the possible contributions of other accelerating mechanisms to the operation of such a device. Some of these possibilities are described in reference 4.

As mentioned, a constriction of the plasma can result from the pinch pressure $j_z B_\theta$ exerted by its own magnetic field on the arc. This effect is considered to be slight in the present investigation because of the absence of the extremely high current density required. Such current densities may occur even at moderate currents in the presence of a cathode spot, but in the present device, emission occurred over a considerable area in the region of the cathode tip. Similarly, the axial force $j_r B_\theta$ is slight because of the small value of B_θ. However, at the lower pressures where small forces can be effective, such mechanisms may not be entirely negligible.

The possibility of a significant contribution by the force $j_\theta B_r$ resulting from the interaction of the azimuthal current with the radial magnetic field component is reduced since, with this configuration, it is possible for the current to follow the magnetic field lines from cathode to anode without crossing the magnetic field lines. Thus, the azimuthal currents are reduced significantly since they are caused by the current component that crosses the magnetic field lines. A further consideration is the difficulty in forcing the current to cross magnetic field lines in $j \times B$ accelerators and Hall current accelerators that rely on such action for the production of the accelerating force. A constant current

arc, which naturally operates in a configuration requiring minimum voltage, has a strong tendency to bow out downstream when forced to cross magnetic field lines so that the radial current flows in a region of lesser magnetic field strength. However, in a system designed to permit unimpeded current flow between the electrodes, it appears unlikely that the arc would choose a configuration that would involve crossing of field lines with the resultant azimuthal current effects.

Another force operative in many plasma devices is that due to a superimposed gas-pressure gradient. This complication was eliminated in the present investigation, which utilized a closed-circuit duct so that the accelerating action actually resulted in a pumping of the gas around the circuit.

A final effect that exists in some plasma accelerators is the centrifugal force that occurs when the plasma rotates under the action of the $j_r B_z$ force. A device in which this mechanism occurred has been tested and the results are reported in reference 8. However, the Mach number, indicated by the ratio of pitot-pressure measurements to static-pressure measurement, decreased as the power was increased, whereas in the present mechanism the Mach number increased when the power increased. This phenomenon of plasma rotation also occurs in a Hall current device as a kind of discontinuity in the operation of the device when the pressure is raised and an anode spot is formed so that the arc forms a discrete column. This effect was observed in the present device when the anode was moved upstream so that j_r and B_z were increased in the anode region and the current was forced to cross the field lines. The formation of an anode spot inevitably resulted in serious sudden damage to the anode, similar to the electrode failure described in reference 9, and consequently no measurements were made under these conditions.

APPARATUS AND PROCEDURE

Vacuum Chamber

A closed-circuit duct was used in order to study the flow produced by the interaction of plasma and magnetic field without the complication of a superimposed gas-pressure gradient. A schematic drawing of the system is shown in figure 1 and a photograph of the system is shown in figure 2. For convenience in making connections to the vacuum system, nonmagnetic stainless-steel tubing was used on each end of the duct system and glass pipe was used for the return ducting. At the magnetic-nozzle location, quartz tubing was used. In order to obtain a strong magnetic field with a minimum of power, the diameter of the quartz tubing was reduced to 4.4 cm to pass through the magnet coil. Downstream of the magnet coil, a short section of boron nitride was used to connect the 4.4-cm tube to a 10-cm tube.

The tubes for the gas inlet and the vacuum pump were located in the return duct of the system so that no flow would be produced through the system prior to starting.

Plasma Accelerator

A schematic diagram of the magnetically confined arc configuration is shown in figure 3. It consisted of a cathode located on the center line of the 4.4-cm quartz tube near the upstream end of the magnet coil. The anode was located downstream of the magnet coil and had a toroidal shape. A photograph of the expansion region with the accelerator in operation is shown in figure 4.

The power required for the direct-current arc was obtained from three arc welders connected in series. The open-circuit voltage of each arc welder was 105 volts, giving a total open-circuit voltage of 315 volts. When the arc started, the voltage decreased to the value required by the current setting, so that no ballast resistors were required to stabilize the arc. The maximum power available from the three arc welders was approximately 50 kilowatts.

When the open-circuit voltage was inadequate to start the arc, a spark discharge from the cathode to the anode was used. The electrical circuit is shown in figure 5. This circuit is similar to the circuit described in reference 10, except that a hydrogen thyratron tube (6279/5C22) was used instead of the double-pole, double-throw switch.

The cathode was a thoriated tungsten rod with a pointed tip. The base of the cathode was water cooled, as shown in figure 1, with a water supply at a pressure of approximately 200 newtons/cm^2 (300 psi). The toroidal-shaped anode was a casting composed of 90 percent silver and 10 percent copper (coin silver). The wall thickness of the anode was approximately 1.59 mm. The anode tubing had a rectangular cross section, as shown in figure 3, and was also water cooled by the high-pressure water supply.

The magnet coil, shown in figure 3, consisted of 32 copper disks cut radially. Each disk was silver soldered to the preceding disk to form a helical solenoid. The coil was enclosed by a water jacket. This coil design offers an easy method of varying the radial current distribution to achieve higher efficiency and is similar to the high-intensity magnetic field coil described in reference 11. The copper disks had an inside diameter of 5.72 cm and an outside diameter of 11.56 cm, and were 0.79 mm thick. The turns of the coil were separated by glass beads of 0.61-mm diameter. The glass beads were glued to one side of the copper disks with electrical varnish, so that the other side of the disks was in direct contact with the cooling water. High-pressure water (200 newtons/cm^2, or 300 psi) entered the water jacket at the inner perimeter of the coil, passed through the coil, and exited radially. This design permitted the coil to be operated continuously at 3100 amperes (the maximum current available) with an increase in water temperature of

about 20° C. The maximum field at the center of the coil was 13 000 gauss at 3100 amperes and 25 volts.

The variations of the magnetic-field ratios B_z/B_0 and B_r/B_0 with radius are shown in figure 6 at five axial locations. It is interesting to note that at the center of the coil (z/L = 0) and at the edge of the coil (z/L = 1) the magnetic field increased with an increase in radius.

Instrumentation and Measurements

A thin plastic vane was placed in the return duct of the vacuum system (fig. 1) as a flow indicator. Photographs of the vane are shown in figure 7 with power off and with power on and the vane deflected.

Static pressure was measured at the wall, 2 cm downstream from the anode, through an orifice with an inside diameter of 0.47 cm. Pitot-pressure measurements were obtained on the center line 3.5 cm downstream from the anode by using a conical water-cooled total-pressure tube with an inside diameter of 0.47 cm, as shown in figures 1 and 3. Static pressure and pitot pressure were measured with thermocouple vacuum gages that were calibrated in argon gas. The accuracy of the gages is estimated to be within 8 percent. The thermocouple pressure sensors were located as near as possible to the vacuum system to reduce the lag time. The metal shields of the thermocouple pressure sensors were grounded, and shielded wiring and filter circuit were used to prevent interference from the arc.

Because of the nature of the flow in a plasma accelerator, the pressure measurements are considered in only a qualitative sense. The pitot-pressure measurements were made in the center of the stream in a continuous flow and are accurate within the accuracy of the instrumentation. The static-pressure measurements contain some error because, for the lower pressure runs, the flow is in either the slip-flow region or the beginning of the region of transition to free-molecule flow. In view of the results of reference 12, the total error due to this cause is believed to be less than 10 percent at low arc currents but somewhat greater at arc currents above 270 amperes, when starting at an initial static pressure of 0.765 mm Hg.

Another factor to be considered is the possible error due to the failure of the static-pressure reading to account for any partial pressure due to the magnetic field in the region of the orifice. If the theoretical capability of the field were actually exerted as pressure in the gas, this magnetic pressure would be of the same order as the gas pressure. However, under similar conditions in reference 5, a theoretical magnetic pressure capability of 15 800 mm Hg produces an actual differential of only about 75 mm Hg in the pressure of a fully ionized arc. Thus it is apparent that the relatively weak field (1500 gauss) would be even less effective in the region of the static orifice, where the

degree of ionization is much lower. This view is supported by the studies reported in references 8 and 13 where, apparently, consistent results were obtained without correcting static-pressure measurements made in a field of even greater strength. Therefore, the effect of the field on the static-pressure reading is considered to be negligible except possibly in the runs at the lowest operating pressures, where the ratio of pitot to static pressure is quite sensitive to slight errors in the static-pressure reading.

The method used to measure the charged-particle velocities is described in reference 10. A luminous disturbance was created in the flow by discharging a 0.5-microfarad capacitor from the cathode to the anode. The electrical circuit used was the same as that employed to start the arc. (See fig. 5.) The capacitor was generally charged to 5000 volts. The change in light intensity was observed through 0.8-mm collimating slits by two photomultipliers at various downstream locations. The photomultipliers were connected to a dual-beam oscilloscope. Since the photomultiplier nearest the anode observed the change in light intensity before the other photomultiplier, the respective oscilloscope traces were displaced. This displacement represents a time lapse that can be used with the known collimator spacing to compute the longitudinal velocity of the charged particles.

Procedure

Pressure measurements were obtained at static pressures from 0.765 mm Hg to 2.60 mm Hg at arc currents up to 390 amperes with the downstream edge of the magnet at three locations: 6.4 mm, 11.1 mm, and 15.9 mm upstream from the anode. The effect of varying the magnetic field strength was determined by operating the magnet at 13 000 gauss, 9300 gauss, and 5200 gauss with the magnet located 11.1 mm from the anode. Some preliminary measurements of charged-particle velocities were obtained at arc currents up to 335 amperes at a static pressure of 0.765 mm Hg with the magnet 11.1 mm from the anode.

The procedure followed in obtaining these data was first to set the initial static pressure of argon gas in the vacuum chamber. The magnet coil was then energized and the arc was started and set at the desired current. Charged-particle velocities were obtained as described in the section entitled "Instrumentation and Measurements." A test generally did not exceed 3 to 5 seconds, since the connection between the arc discharge tube and the boron nitride connector (fig. 3) was not water cooled and, when overheated, the rubber seal would begin to leak.

RESULTS

In figure 8 the variation of arc voltage, pitot pressure, and wall static pressure with arc current is presented at magnetic fields of 13 000 gauss, 9300 gauss, and 5200 gauss. The variation of the pressure ratio p_t/p with arc current and the variation of the arc

power with arc current are presented in figures 9 and 10, respectively, at magnetic fields of 13 000 gauss, 9300 gauss, and 5200 gauss. For the tests from which the data of figures 8, 9, and 10 were obtained the initial static pressure was 0.765 mm Hg; the anode was 11.1 mm from the downstream edge of the magnet.

The variations of arc voltage, pitot pressure, and wall static pressure with arc current are shown in figure 11 for initial static pressures from 0.765 mm Hg to 2.600 mm Hg and for three anode locations with a magnetic field of 13 000 gauss. The variation of the pressure ratio p_t/p with arc current and the variation of arc power with arc current are presented in figures 12 and 13, respectively, for the same three anode locations and initial static pressures. Measurements of the charged-particle velocities obtained at two locations, 10.5 cm and 18.5 cm downstream from the anode, with an initial static pressure of 0.765 mm Hg and with arc currents up to 335 amperes, are presented in figure 14. Some typical oscilloscope traces obtained with the photomultipliers are given in figure 15.

DISCUSSION

Design and Operation

In this experiment the cathode was located near the center of the magnetic field coil and a toroidal anode was located outside the coil as shown in figure 16. At the center of the coil, where the magnetic field was a maximum, the arc was constricted, and then the arc expanded out to the circular anode by following the magnetic field lines. Since current density is quite high in the constricted portion of the arc, the neutral particles that diffuse into the arc column are ionized and trapped by the magnetic field. This increases the pressure and density in the arc and causes a radial pressure gradient to develop in the discharge tube. This process is described in reference 14, and has been visually observed and measured in the experiment of reference 5.

As the arc column expands downstream, the current density is less and the radial pressure gradient decreases. As a result, there is a longitudinal pressure gradient in the arc column from the cathode to the anode, causing a longitudinal flow that expands through the center of the circular anode.

This design has some similarity to the magnetic-mirror device used in the fusion experiments with the magnetic bottle described in reference 15. The magnetic mirror is produced at the cathode where the increase in magnetic field exerts a force that reflects the charged particles toward the anode and allows them to escape downstream.

Characteristics of Accelerator

The pressures measured in the plasma flow are average values resulting from the low-velocity neutral gas and the high-velocity charged particles. The flow is not in

equilibrium at low static pressures and the specific-heat ratio is not accurately known. Only the trends of the pressure data are considered in the analysis. When the arc is started without the magnetic field, both the pitot pressure and the static pressure increase because of the increase in temperature in the vacuum chamber; and no flow is initiated through the system. When the arc is started with the magnetic field energized, the radial heat conduction from the arc is reduced and the arc is constricted near the cathode. The current density and arc temperature are higher in the more constricted region and a longitudinal pressure gradient develops in the arc column. As a result, the pitot pressure increases and the static pressure decreases, as indicated in figures 8 and 11.

The effect of varying the magnetic field and the arc current is shown in figure 9. For a given arc current, increasing the magnetic field increases the ratio of pitot pressure to static pressure. At an arc current of 210 amperes, increasing the magnetic field from 5200 gauss to 13 000 gauss increased the pressure ratio about 300 percent from 3.30 to 9.50. At a higher arc current of 340 amperes, with the same increase in magnetic field, the pressure ratio increased about 450 percent from 4.60 to 20.60. Since the pressure in the magnetically confined arc column is a function of B^2 (p. 48 of ref. 7), the increase in pressure ratio, indicating an increase in Mach number with an increase in magnetic field and arc current, is attributed to the reduction in radial heat conductivity from the arc column and to the constriction of the arc, which increases the pressure, current density, and arc temperature. Theory (ref. 5) indicates that at sufficiently high arc temperatures (above about 15 000° K), the reduction in the radial heat conductivity due to an axial magnetic field superimposed on the arc column is inversely proportional to the 5/2 power of the temperature.

Comparison of figures 12(a), 12(b), 12(c), and 12(d), at a given arc current, indicates that increasing the initial pressure in the vacuum system reduces the ratio of pitot pressure to static pressure from the accelerator, indicating a reduction in Mach number. This effect is probably due to the increase in mass which must be accelerated and to the increase in radial heat conductivity from the arc column, since the magnetic field is less effective at the higher pressures. It appears that the capability of the accelerator, as indicated by the pressure measurements, decreased with an increase in the operating pressure.

The effect of varying the anode location on the ratio of pitot pressure to static pressure is also shown in figure 12. At the higher arc currents the pressure ratio increased when the distance of the anode from the magnet was changed from 11.1 mm to 6.4 mm. However, with lower arc currents and at the lower pressures (fig. 12(a)), the pressure ratio decreased when the anode was moved nearer the magnet through the same range. With the anode at the optimum location, the arc is expected to expand smoothly to the anode by following the magnetic field lines. Moving the anode closer to the magnet coil

than the optimum position would force the arc to cross the magnetic field lines, spin the arc and rotate the plasma, and interfere with the smooth expansion of the flow.

Since moving the anode nearer the magnet coil increased the pressure ratio at the higher arc currents, the anode was next located even with the end of the magnet coil. Each time the device was operated with the anode in this location, the anode was punctured on the downstream side. The same type of electrode failure is described in reference 9, in which a long arc with currents up to 180 amperes was operated in a uniform magnetic field. When the gas pressure was lowered during operation at a high power input, a spot formed on the anode on the side most remote from the cathode, puncturing the anode. It appears that the optimum anode location is dependent on the arc current as well as on other parameters such as the magnetic field strength, the pressure, and the dimensions of the anode.

The maximum pressure ratio obtained in this investigation was 40 (see fig. 12), indicating that a hypersonic flow can be obtained with this device. This result was obtained with the maximum arc current and magnetic field available and at the lowest pressure. At initial static pressures from 0.765 mm Hg to 1.30 mm Hg, with arc current from 176 to 390 amperes, the pressure ratio exceeded 2.80. This result indicates that within a certain range of parameters a supersonic flow can be obtained with the magnetic-nozzle device.

The data in figure 9 indicate that the pressure ratio increased with an increase in the strength of the magnetic field, and the data in figure 12 indicate that for initial static pressures up to 1.30 mm Hg, the pressure ratio increased with an increase in arc current. In neither case does the pressure ratio seem to have reached a limiting value. In general, it appears that with an arc power supply having a higher current and power capability and with a stronger magnetic field, the pressure ratio would continue to increase and supersonic flow could be obtained at higher pressures.

Voltage and Power Characteristics

Some voltage measurements across the arc were obtained under various conditions. The arc voltage (fig. 8), the pressure ratio (fig. 9), and the arc power (fig. 10) increased when the magnetic field strength and the arc current were increased. Decreasing the initial static pressure and, in general, moving the anode toward its optimum location also increased the arc voltage (fig. 11), the pressure ratio (fig. 12), and the arc power (fig. 13). In general, when an increase in pressure ratio occurred in the accelerator, the voltage at constant current also increased to supply the additional power for accelerating the gas. Consequently, the magnetic-nozzle device exhibits a rising volt-ampere characteristic similar to that of most confined arcs, whereas unconfined arcs generally have a falling volt-ampere characteristic. A rising volt-ampere characteristic is desirable for

stabilizing the arc power circuits so that the losses associated with the use of ballast resistors are avoided.

Competing mechanisms influence the arc current-voltage characteristics. In general, if there is an abundance of particles to be ionized, an increase in current tends to cause an increase in conductivity with a consequent drop in arc voltage. However, this effect is at least partially offset if the increase in current causes a large increase in the acceleration of charged particles out of the arc plasma so that the ionization of an even greater number of particles is required. Finally, if the particle density is sufficiently low, the additional ionization needed because of the increase in current and the acceleration of ionized particles from the arc is supplied by multiple ionization. The arc described in reference 5, which utilized a higher pressure and smaller charged-particle ejection rate than the present device, had a falling characteristic. In the present investigation, this condition was approached in the highest pressure (2.60 mm Hg) mode of operation (fig. 11(b)). However, all other experiments were characterized by a definite increase of voltage with current, thereby indicating the influence of the ejection of charged particles together with the decrease in the particle density on the conductivity of the arc.

In the present investigation, increasing the magnetic field strength at constant current resulted in an increase in arc voltage. In contrast, in the investigation described in reference 5 the arc operated in a magnetic field which was essentially uniform so that increasing the field strength simply resulted in a decrease of the energy loss due to radial heat conduction. However, in the present device, this phenomenon is more than offset by the effect of the strong longitudinal gradient of the field, an effect that increases the loss of energy from the arc by pumping charged particles out of it.

Velocity Measurements

Measurements of charged-particle velocities are shown in figure 14 for two locations of the measurement photocells. At positions nearer the anode, because of the high degree of ionization in the plasma flow, it was difficult to obtain velocity measurements by creating a luminous disturbance in the flow and measuring its time of flight over a known distance with photomultipliers. As shown in figure 15(a), the increase in ionization from the spark discharge could not be discerned in the plasma flow by the photomultiplier located nearest the anode. Downstream from the anode, the signal from the spark discharge is more clearly defined (figs. 15(b) and 15(c)) but the signal is expanding somewhat as it moves downstream.

Figure 14 shows that the charged-particle velocities increase with an increase in arc current. For a given arc current, the velocity decreases with an increase in distance from the anode since the plasma attains its maximum expansion and velocity slightly downstream of the anode and then immediately begins "shocking down" toward the relatively

low subsonic speed of circulation around the duct. The highest measured charged-particle velocity was 7300 meters/sec with an arc current of 335 amperes. Such velocities are definitely indicative of supersonic flow inasmuch as the sound speed in this region is certainly less than 1900 meters/sec, the approximate value of the speed of sound in argon at 11 000° to 12 000° K when essentially all the particles are ionized. Charged-particle velocities were not obtained at the higher arc currents; because of the increase in luminosity of the flow, the signal from the photomultipliers decreased with an increase in arc current until the signal could no longer be discerned in the flow by the first photomultiplier.

CONCLUSIONS

From an experimental investigation of a plasma accelerator using a dc arc in conjunction with a dc magnetic field to provide a high-temperature plasma flow, the following conclusions were obtained:

1. Pressure measurements, together with direct velocity measurements, indicated that within a certain range of parameters a supersonic flow was obtained.

2. These measurements indicated that with an increase in magnetic field strength and arc current, the velocity increased. With an increase in pressure, the velocity decreased. The maximum pressure ratio obtained was 40.

3. Measurements of charged-particle velocity with photoelectric detectors indicated that the maximum velocity occurred immediately downstream of the anode. The maximum velocity measured was 7300 meters/sec at 10.5 cm from the anode with arc current somewhat less than the maximum obtainable. Because of difficulty with the measuring technique, velocities were not obtained near the anode or at the higher arc currents.

4. The trend of the data indicates that with an arc power supply having a higher current and power capability and with a stronger magnetic field, the pressure ratio would continue to increase, and supersonic flow could be obtained with higher initial static pressures.

Langley Research Center,
National Aeronautics and Space Administration,
Langley Station, Hampton, Va., January 24, 1969,
129-02-08-01-23.

REFERENCES

1. Rudin, Morton: Magnetic Channeling and the Nozzle. [Preprint] 902-59, Amer. Rocket Soc., Aug. 1959.

2. Kuriki, Kyoichi: An Experimental Study on a Plasma Flow Through a Magnetic Nozzle. Rep. No. 380, Aeronaut. Res. Inst., Univ. of Tokyo, Mar. 1964.

3. Jacquelin, M.-H.: Réalisation et étude d'un écoulement continu de plasma dans une tuyère en présence d'un champ magnétique axial. Publ. No. 391, Publ. Sci. Tech. Min. Air (Paris), Feb. 1963.

4. Domitz, Stanley; Kosmahl, H. G.; Ramins, Peter; and Stevens, N. John: Survey of Electromagnetic Accelerators for Space Propulsion. NASA TN D-3332, 1966.

5. Mahn, C.; Ringler, H.; Wienecke, R.; Witkowski, S.; and Zankl, G.: Experimente zur Erhöhung der Lichtbogentemperatur durch Reduktion der Wärmeleitfähigkeit in einem Magnetfeld. Z. Naturforsch., Bd. 19a, Heft 10, Oct. 1964, pp. 1202-1207.

6. Maecker, H.: Plasmaströmungen in Lichtbögen infolge eigenmagnetischer Kompression. Z. Phys., Bd. 141, Heft 1/2, 1955, pp. 198-216.

7. Thompson, W. B.: An Introduction to Plasma Physics. Pergamon Press, c.1962.

8. Grossmann, William, Jr.: Theory and Experiment of a Co-Axial Plasma Accelerator. Ph. D. Thesis, Virginia Polytech. Inst., May 1964.

9. Flowers, J. W.: Electrode Breakdown and Shielding of Intense Discharges Across the Magnetic Field. ORNL-2710 (Contract No. W-7405-eng-26), U.S. At. Energy Com., Apr. 13, 1960.

10. Beasley, W. D.; Brooks, J. D.; and Barger, R. L.: Direct Velocity Measurements in Low-Density Plasma Flows. NASA TN D-1783, 1963.

11. Kolm, Henry H.; and Freeman, Arthur J.: Intense Magnetic Fields. Sci. Amer., vol. 212, no. 4, Apr. 1965, pp. 66-78.

12. Enkenhus, K. R.: The Design, Instrumentation, and Operation of the UTIA Low Density Wind Tunnel. Rep. No. 44 (AFOSR-TN-58-22, AD 148 061), Inst. Aerophys., Univ. of Toronto, June 1957.

13. Cann, G. L.; and Harder, R. L.: Follow-On Investigation of a Steady State Hall Current Accelerator. NASA CR-54062, 1964.

14. Barnett, C. F.; Bell, P. R.; Luce, J. S.; Shipley, E. D.; and Simon, A.: The Oak Ridge Thermonuclear Experiment. Proceedings of the Second United Nations International Conference on the Peaceful Uses of Atomic Energy, Vol. 31 – Theoretical and Experimental Aspects of Controlled Nuclear Fusion, 1958, pp. 298-304.

15. Fowler, T. K.; and Post, Richard F.: Progress Toward Fusion Power. Sci. Amer., vol. 215, no. 6, Dec. 1966, pp. 21-31.

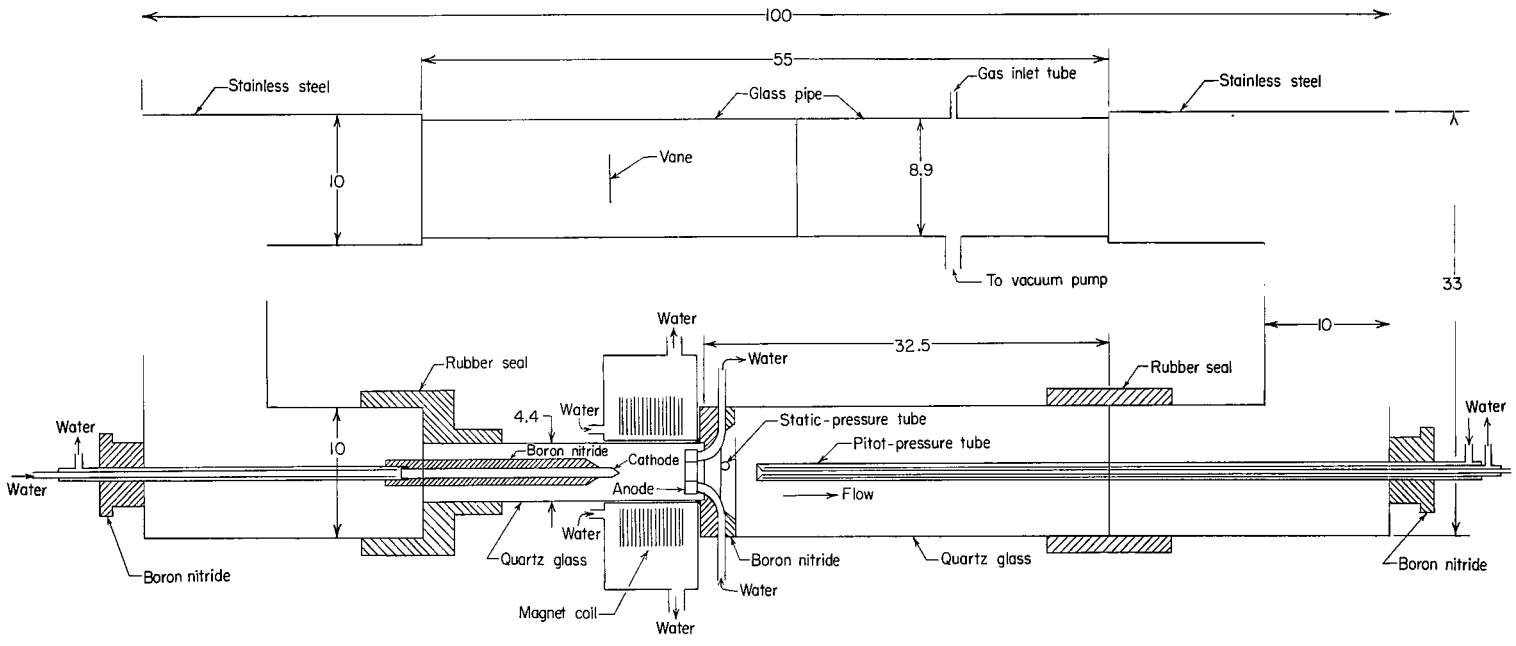

Figure 1.- Schematic diagram of the closed-circuit duct system. All dimensions are in centimeters.

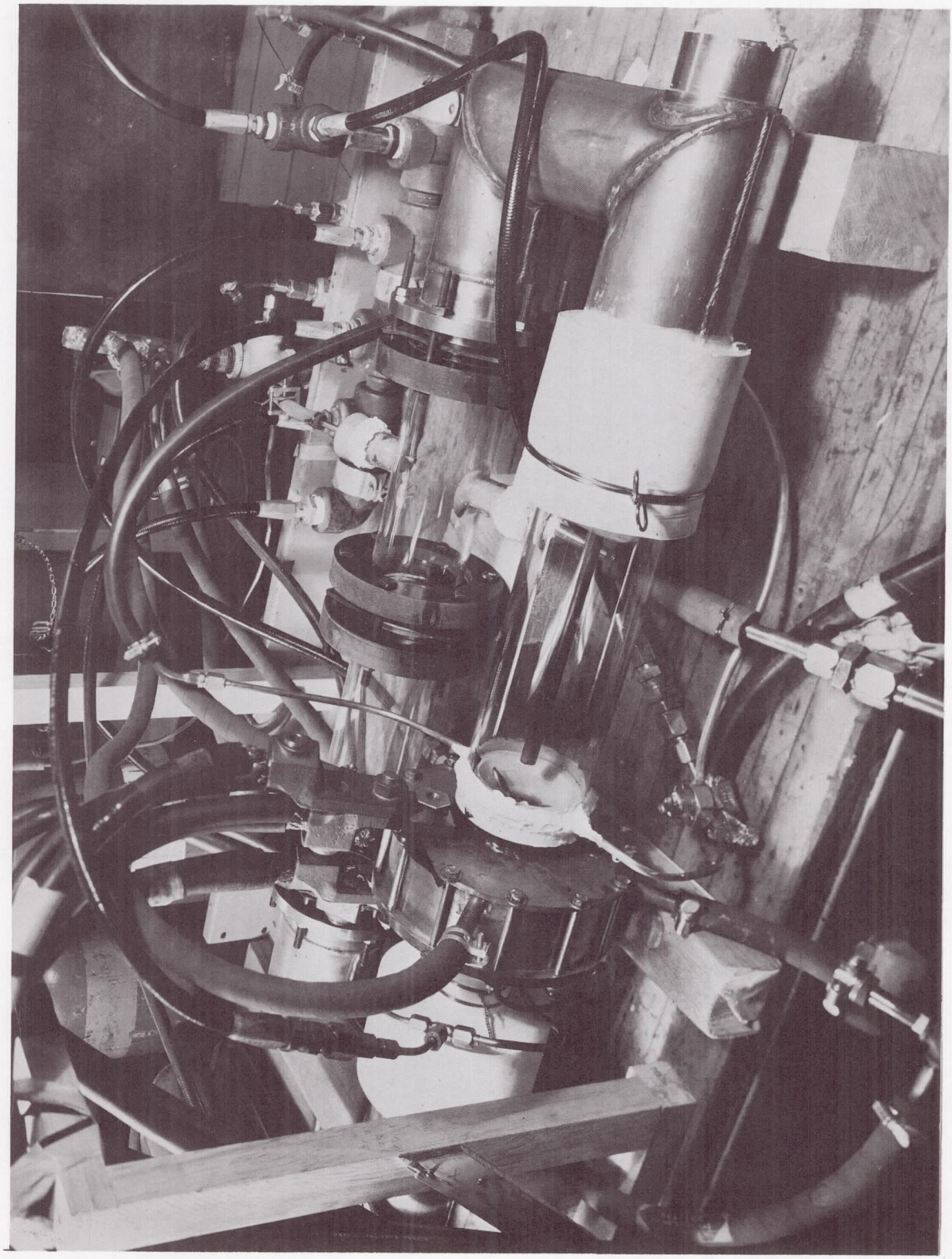

Figure 2.- Photograph of the plasma system.

L-65-7246

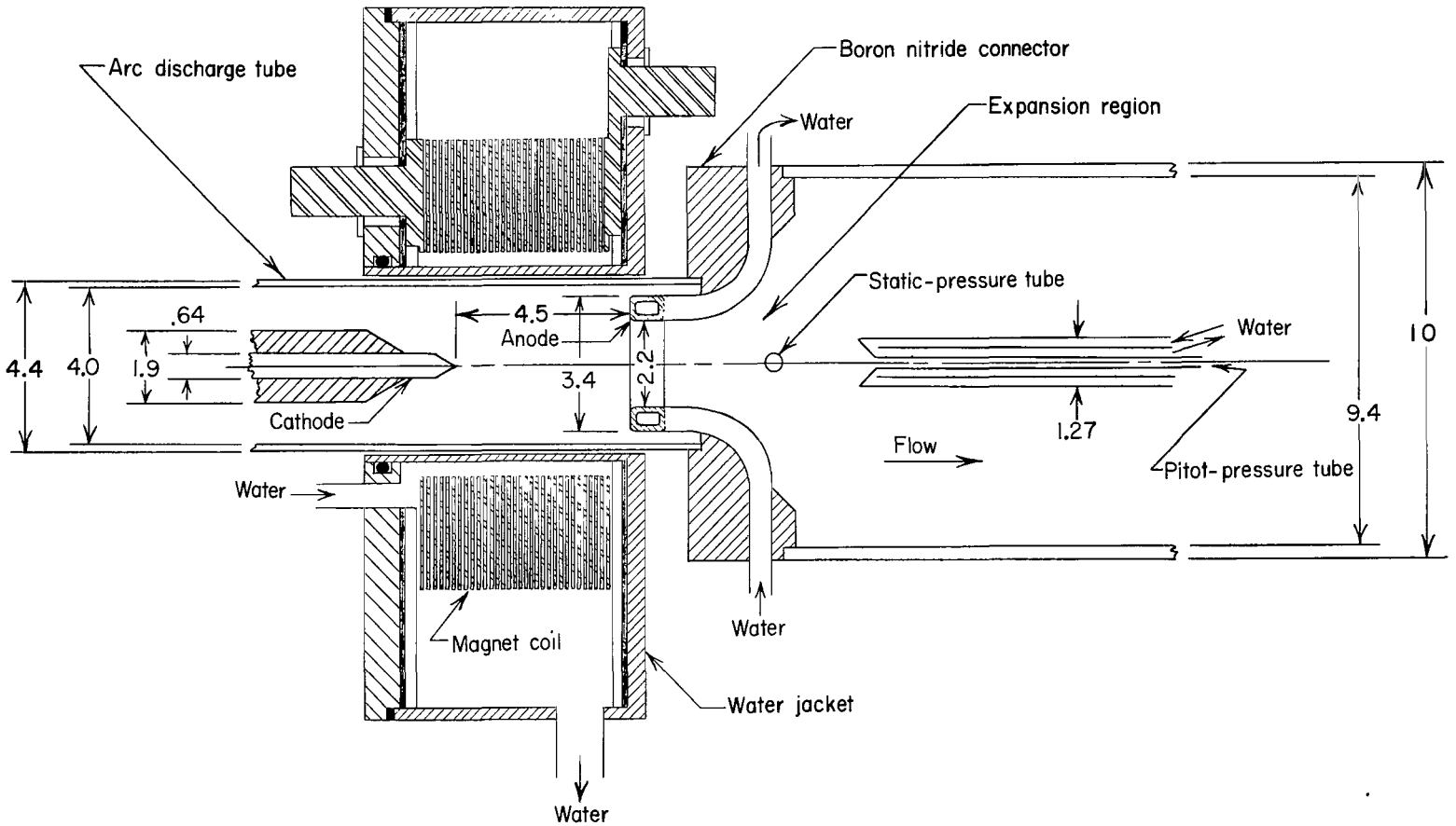

Figure 3.- Schematic diagram of the magnetic-nozzle device. All dimensions are in centimeters.

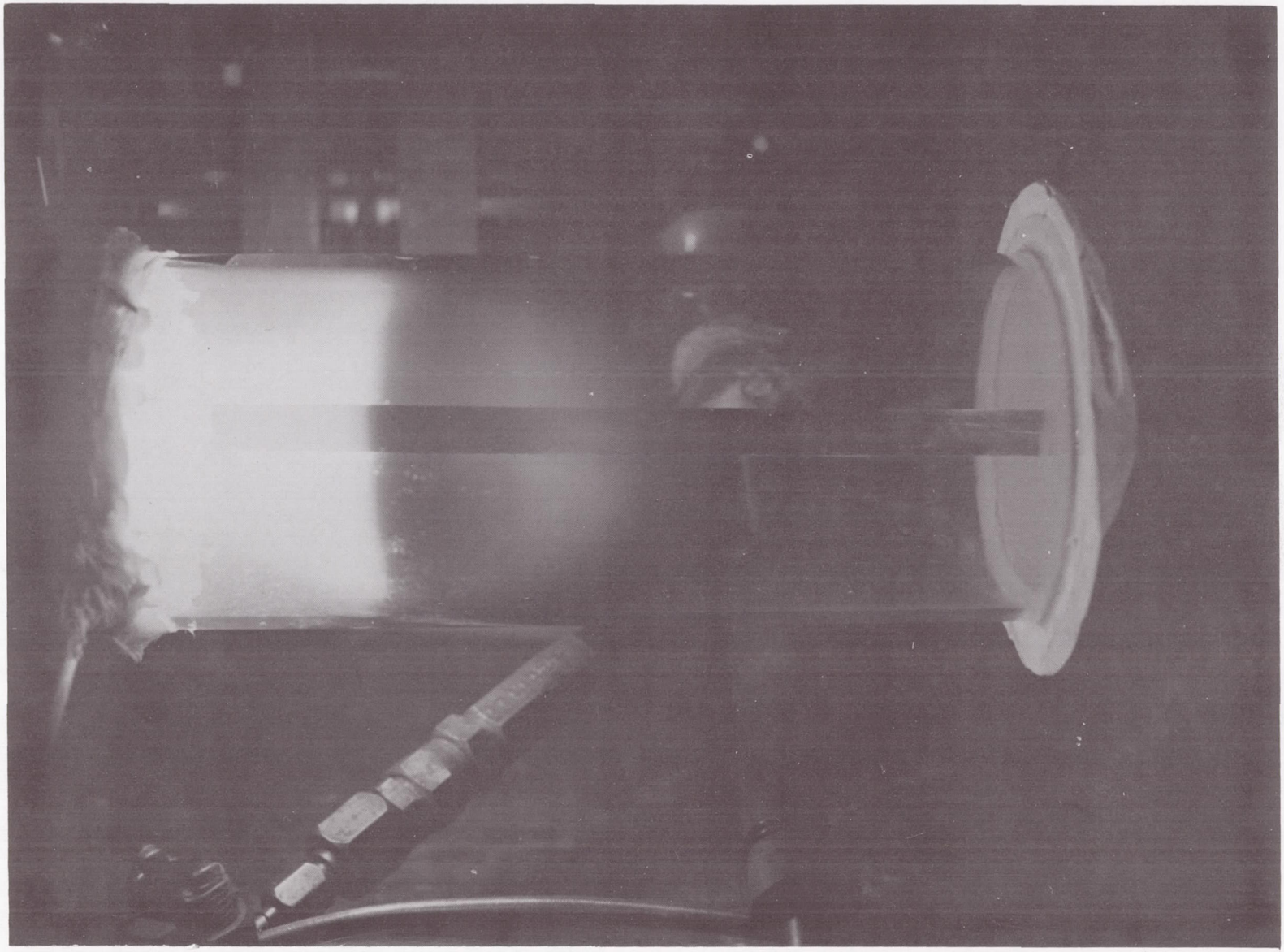

Figure 4.- Photograph of the magnetic-nozzle device in operation. L-69-1216

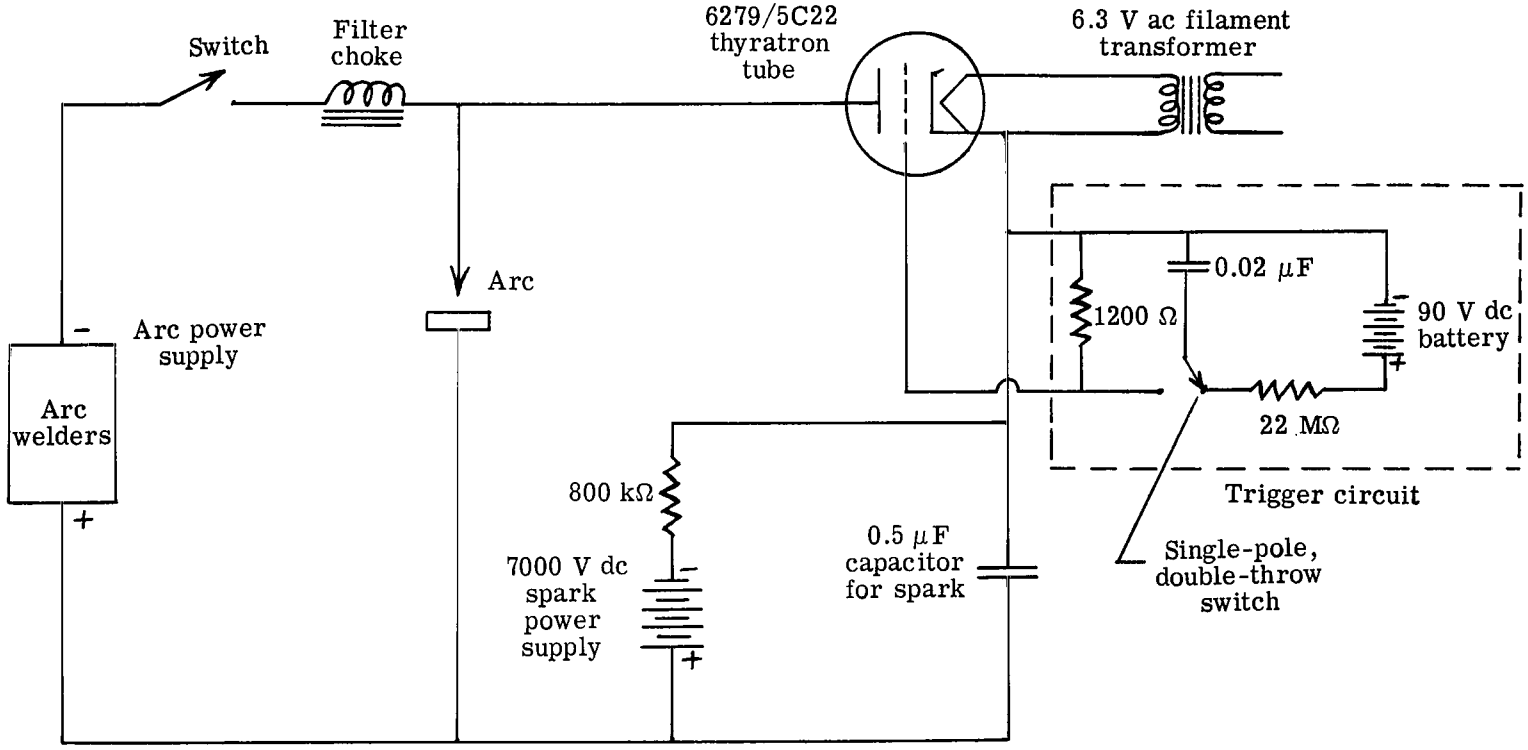

Figure 5.- Electrical circuit.

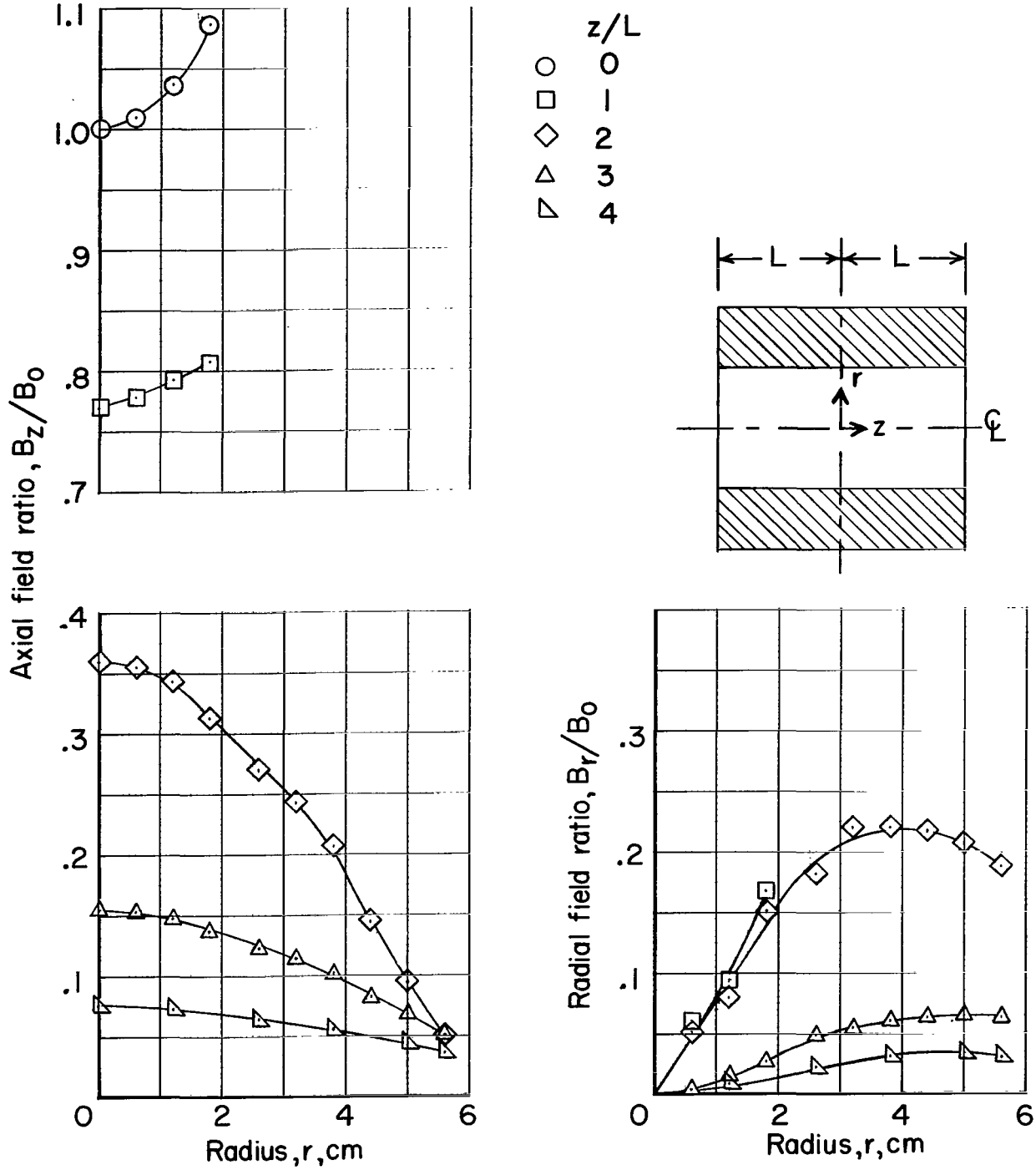

(a) Axial field.

(b) Radial field.

Figure 6.- Variation of the axial and radial magnetic field ratios as a function of radius for various axial locations.

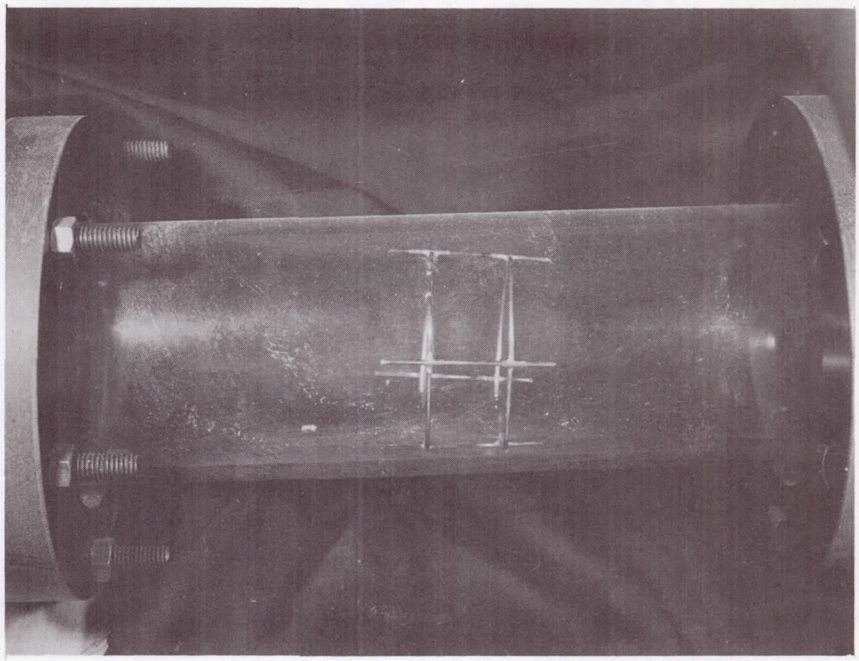

Power off

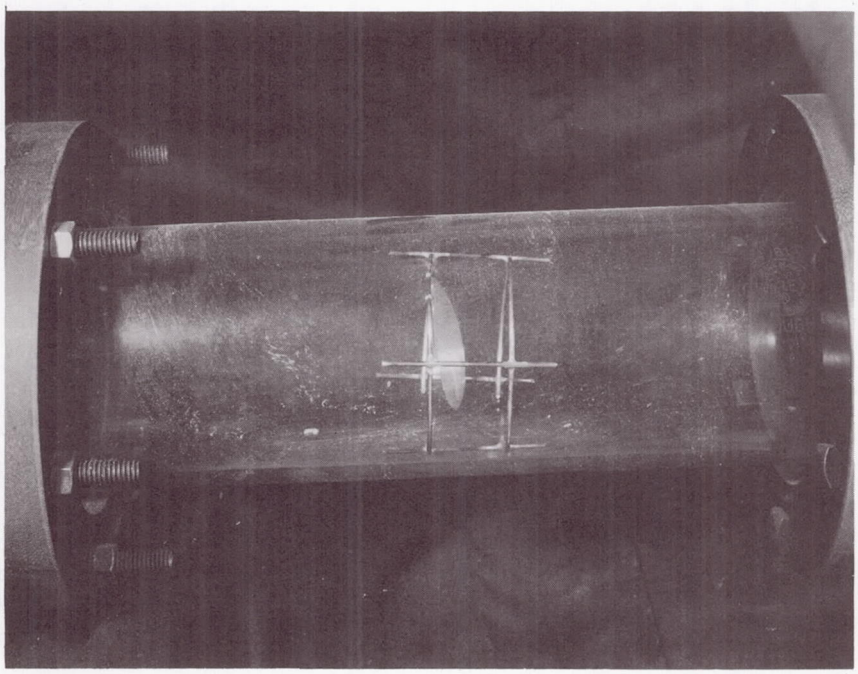

Power on

Figure 7.- Photographs of the vane in the return duct. L-69-1217

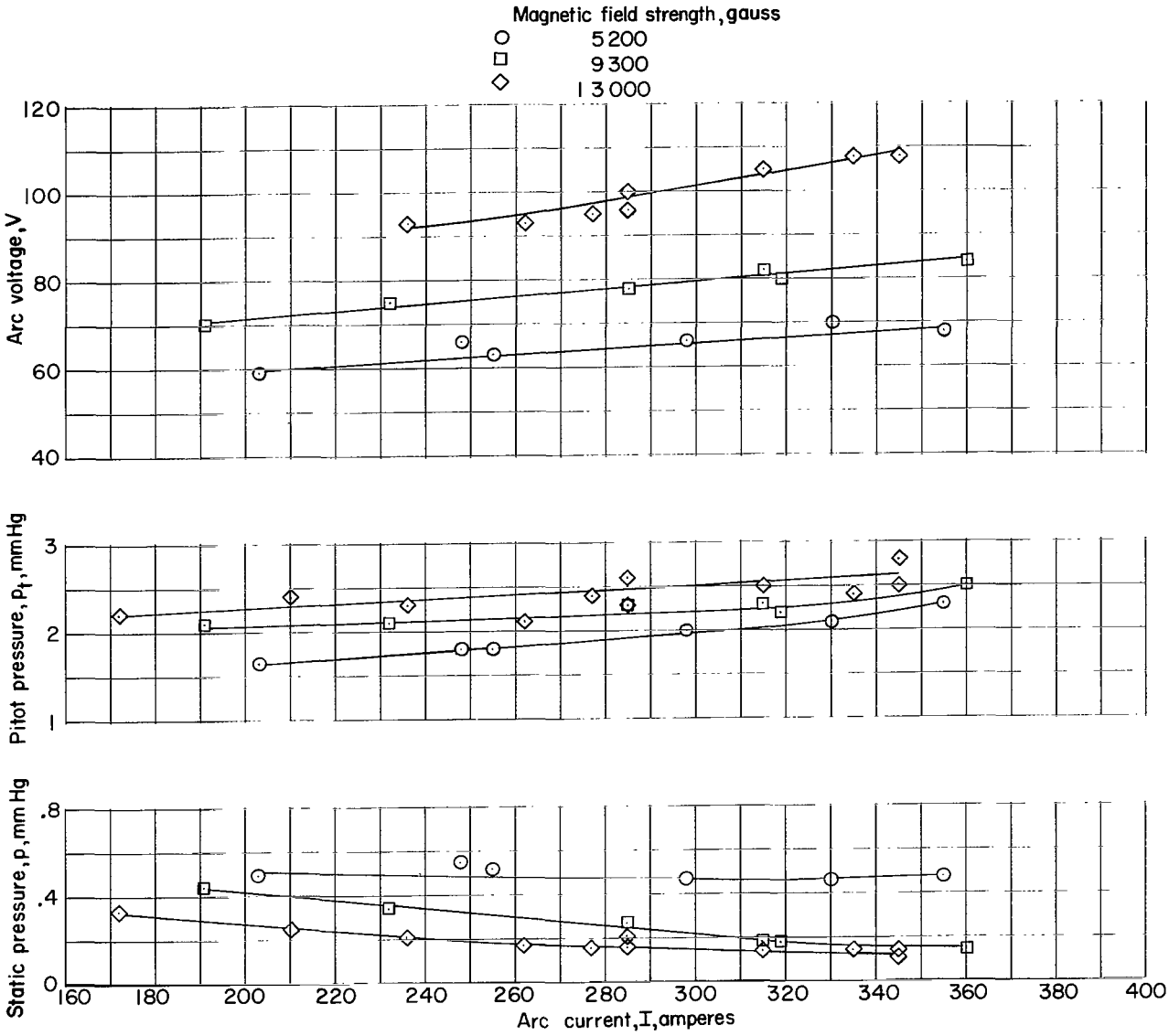

Figure 8.- Variation of arc voltage, pitot pressure, and wall static pressure as a function of arc current with magnetic fields of 13 000 gauss, 9300 gauss, and 5200 gauss at an initial static pressure of 0.765 mm Hg with the anode 11.1 mm from magnet.

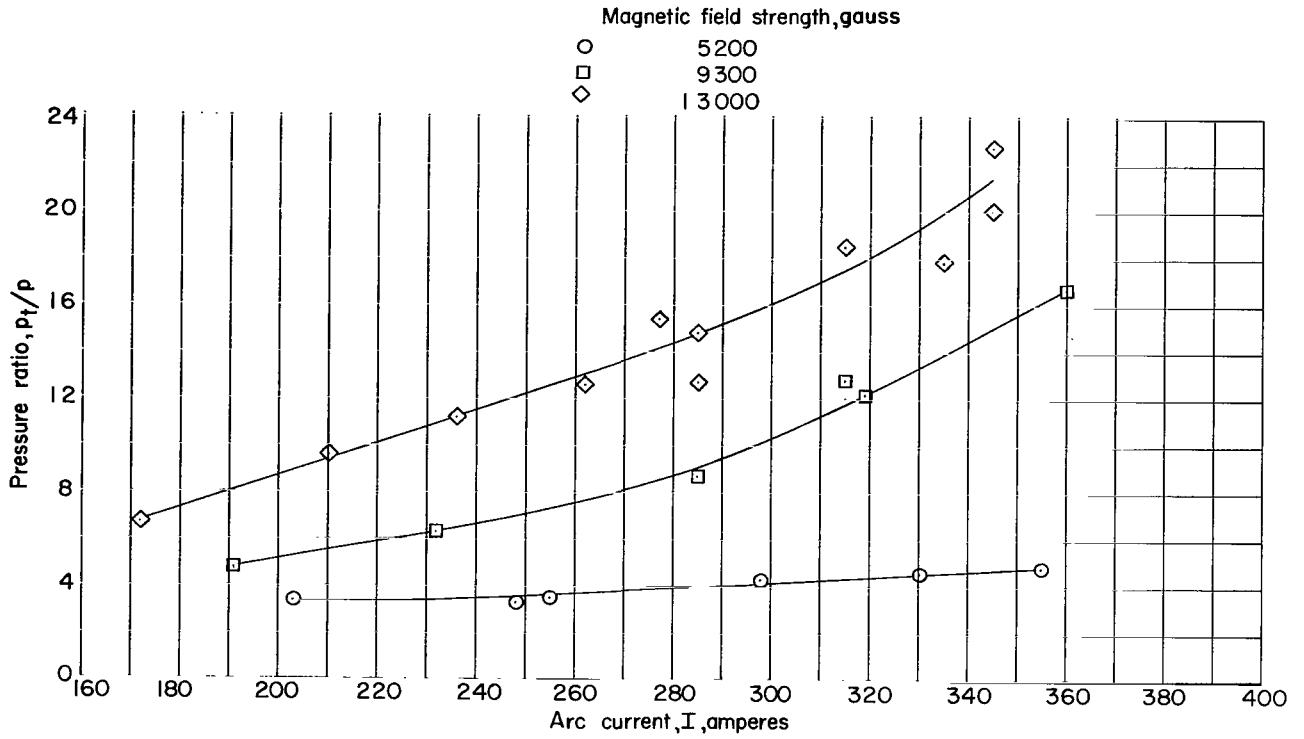

Figure 9.- Variation of the ratio of pitot pressure to static pressure as a function of arc current with magnetic fields of 13 000 gauss, 9300 gauss, and 5200 gauss at an initial static pressure of 0.765 mm Hg with the anode 11.1 mm from magnet.

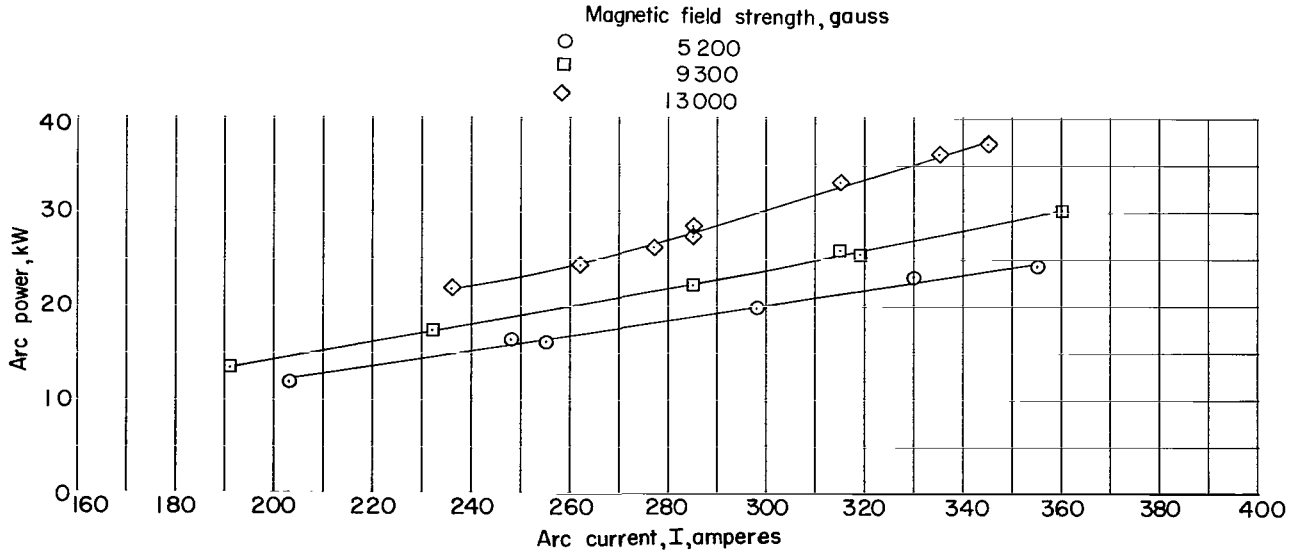

Figure 10.- Variation of arc power as a function of arc current with magnetic fields of 13 000 gauss, 9300 gauss, and 5200 gauss at an initial static pressure of 0.765 mm Hg with the anode 11.1 mm from the magnet.

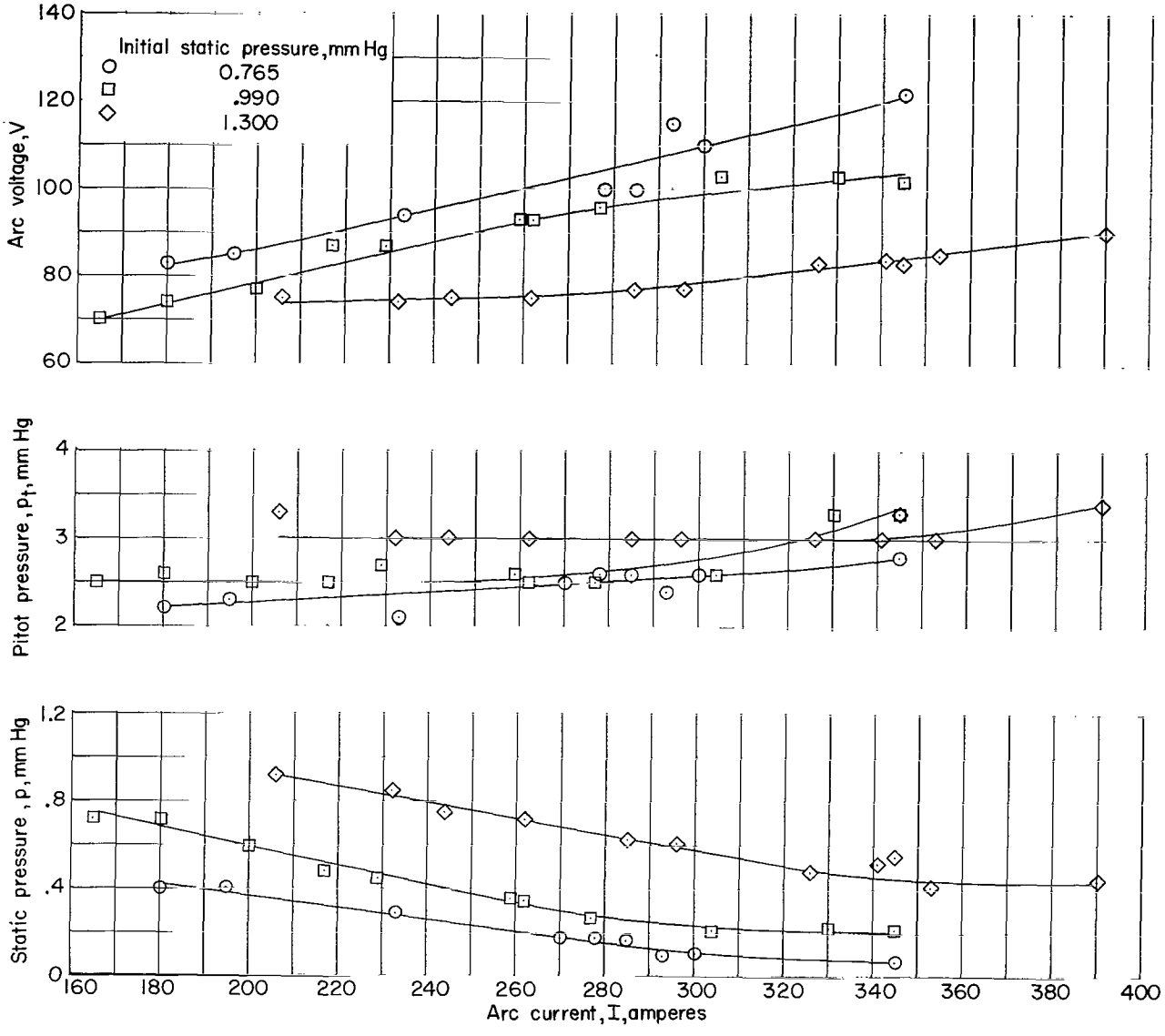

(a) Anode 6.4 mm from magnet.

Figure 11.- Variation of arc voltage, pitot pressure, and wall static pressure as a function of arc current for three anode locations with a magnetic field of 13 000 gauss.

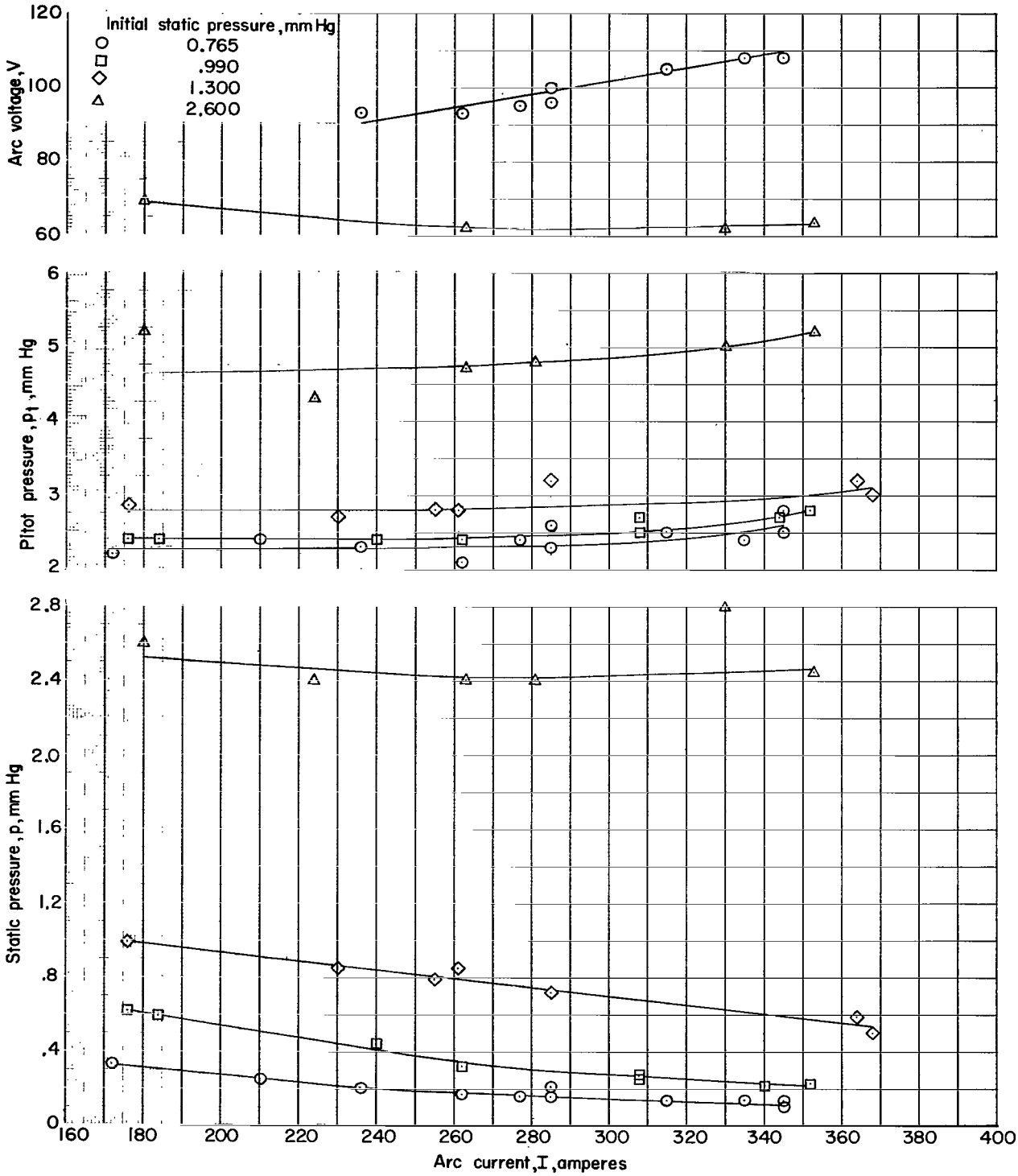

(b) Anode 11.1 mm from magnet.

Figure 11.- Continued.

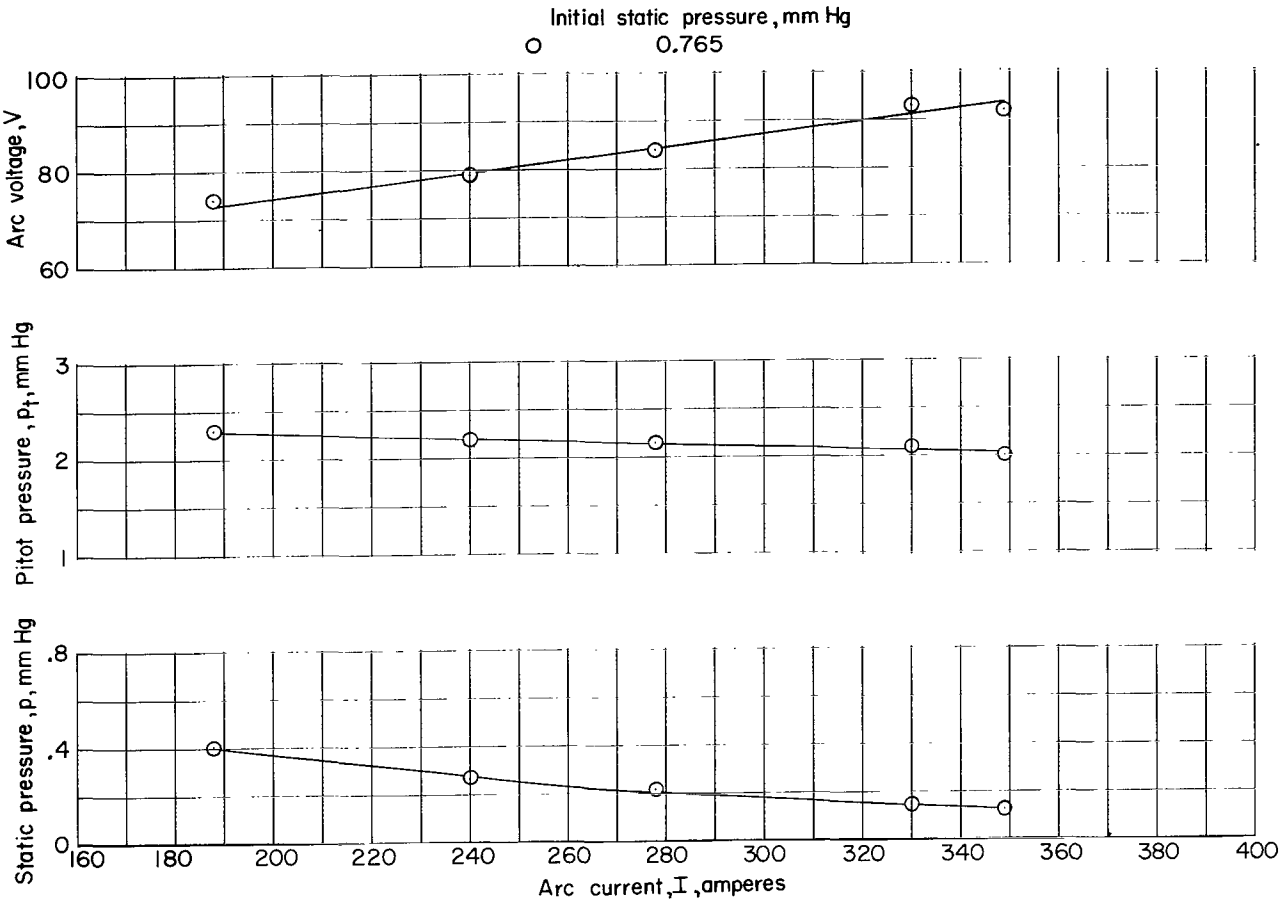

(c) Anode 15.9 mm from magnet.

Figure 11.- Concluded.

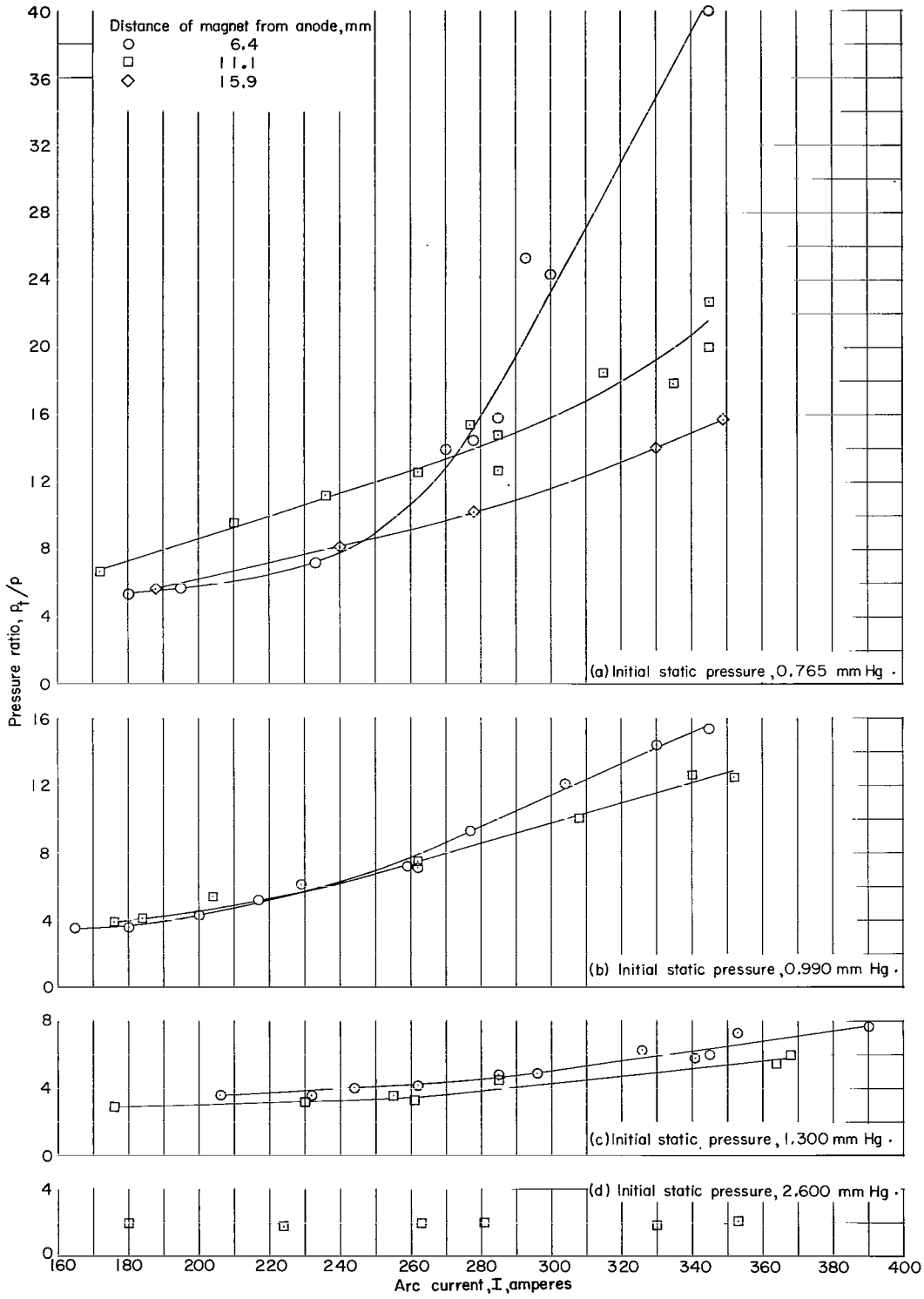

Figure 12.- Variation of the ratio of pitot pressure to static pressure as a function of arc current for three anode locations with a magnetic field of 13 000 gauss.

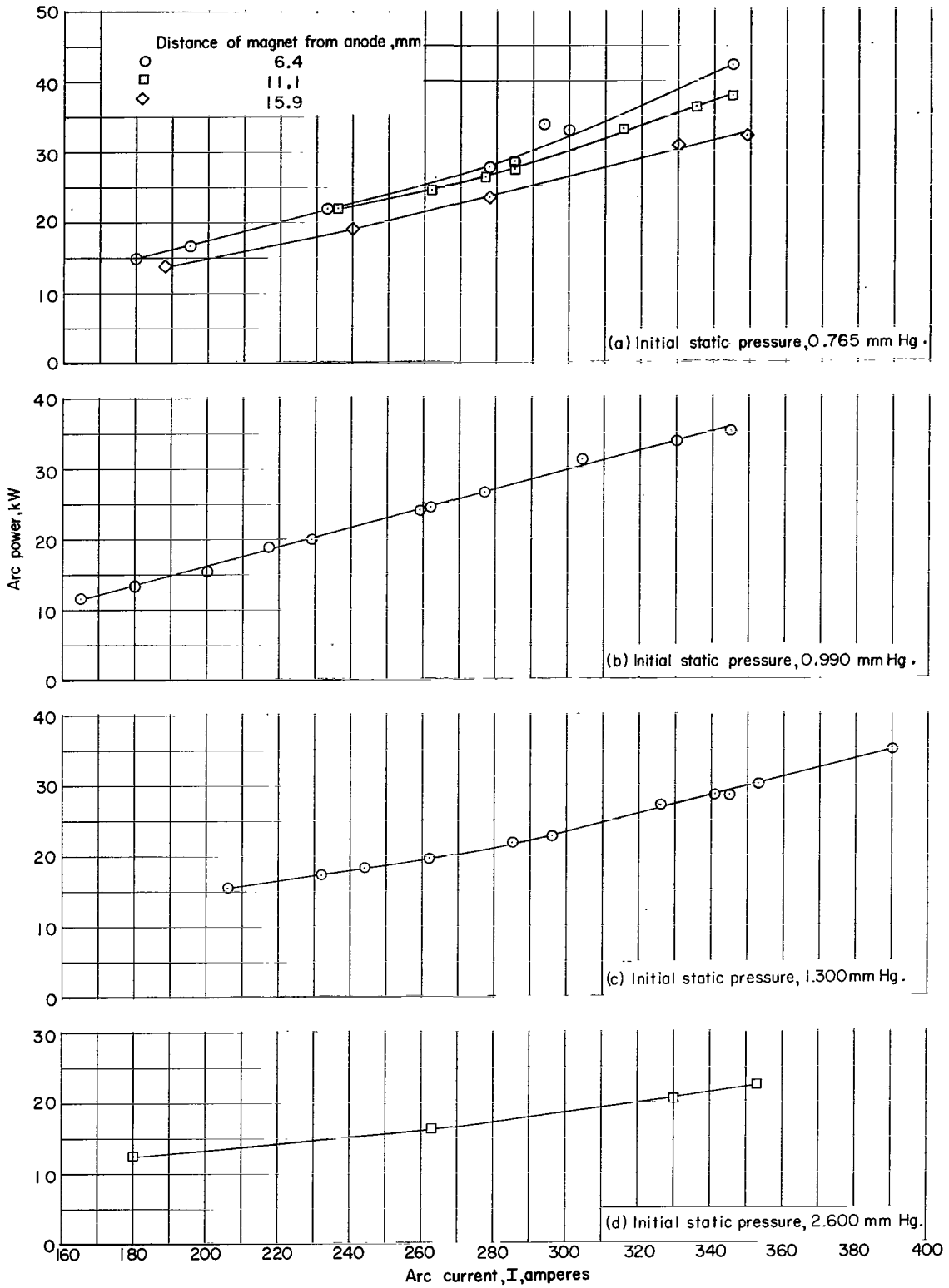

Figure 13.- Variation of arc power as a function of arc current for three anode locations with a magnetic field of 13 000 gauss.

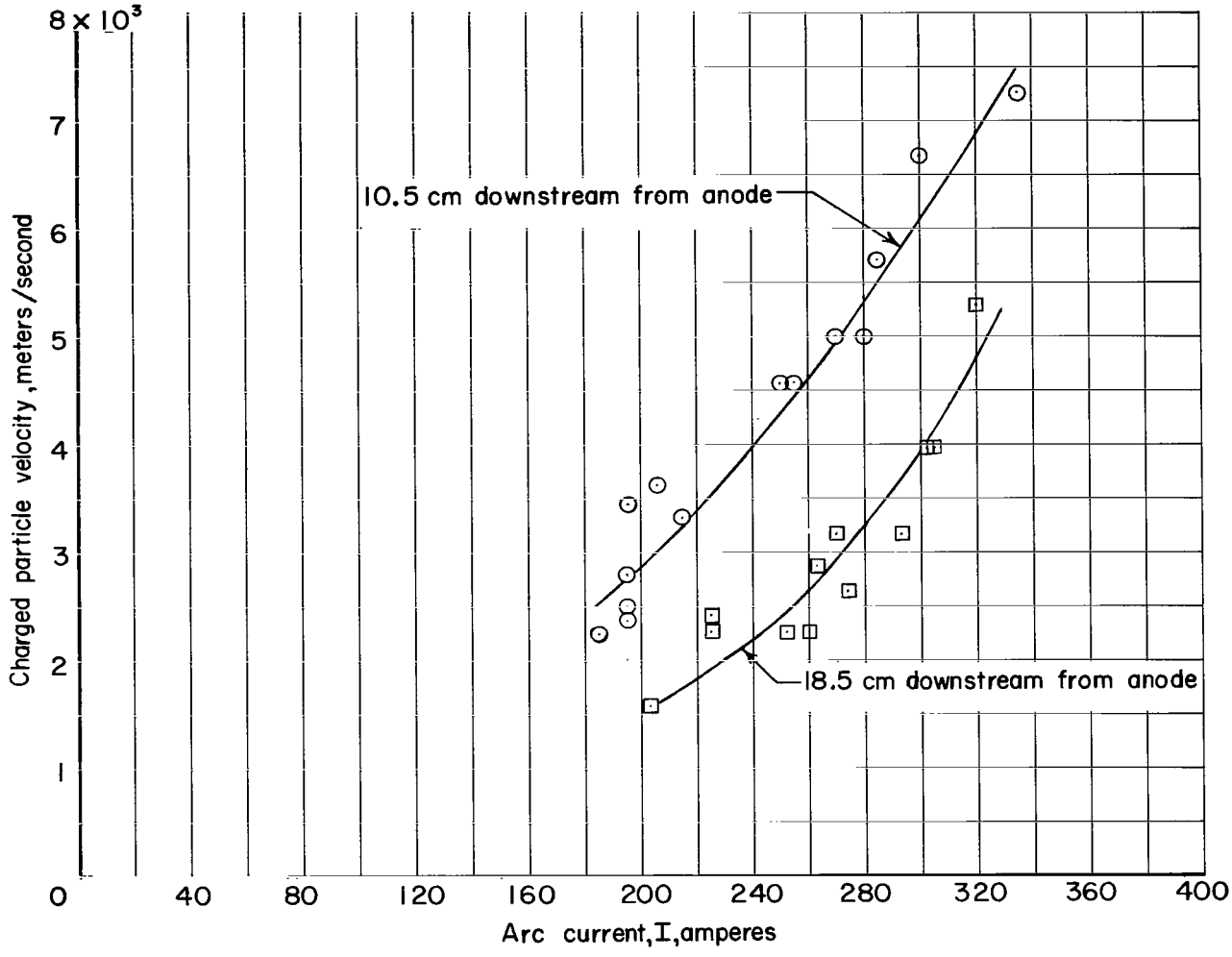

Figure 14.- Variation with arc current of charged-particle velocity at distances of 10.5 cm and 18.5 cm from anode. Anode is 11.1 mm from magnet; magnetic field, 13 000 gauss; initial static pressure, 0.765 mm Hg.

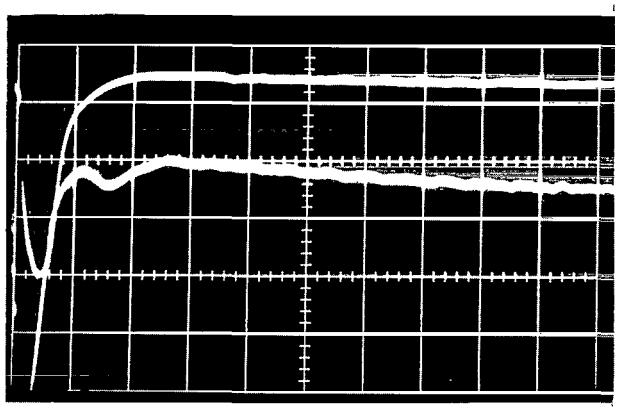

(a) Upstream photomultiplier 6.0 cm from anode; arc current, 180 amperes; photomultiplier spacing, 3.2 cm; oscilloscope sweep, 10 μsec/cm.

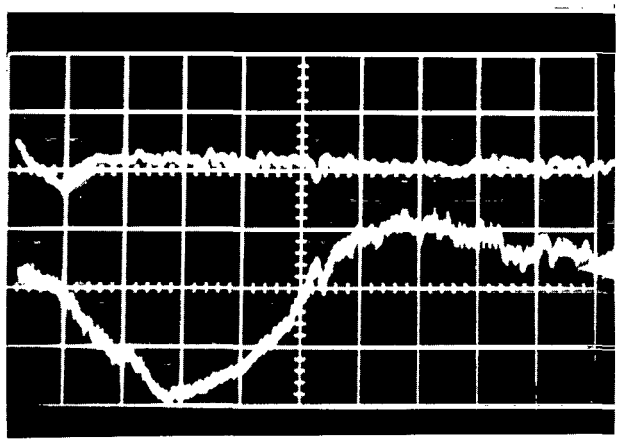

(b) Upstream photomultiplier 10.5 cm from anode; arc current, 185 amperes; photomultiplier spacing, 4.0 cm; oscilloscope sweep, 10 μsec/cm.

18 μsec displacement

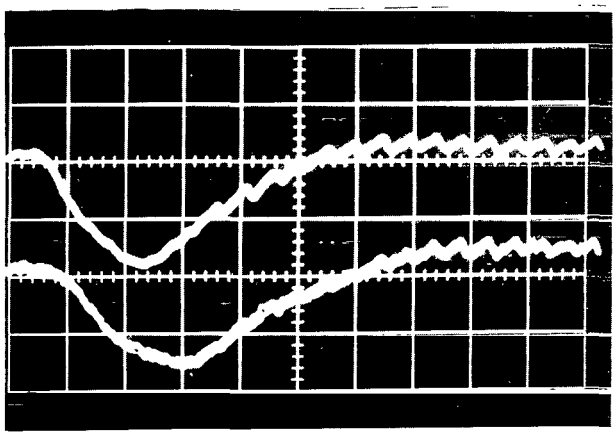

(c) Upstream photomultiplier 18.5 cm from anode; arc current, 225 amperes; photomultiplier spacing, 3.2 cm; oscilloscope sweep, 20 μsec/cm.

14 μsec displacement

L-69-1218

Figure 15.- Typical oscilloscope traces obtained with two photomultipliers placed longitudinally along the direction of flow. Anode is 6.4 mm from magnet; magnetic field, 13 000 gauss; initial static pressure, 0.765 mm Hg.

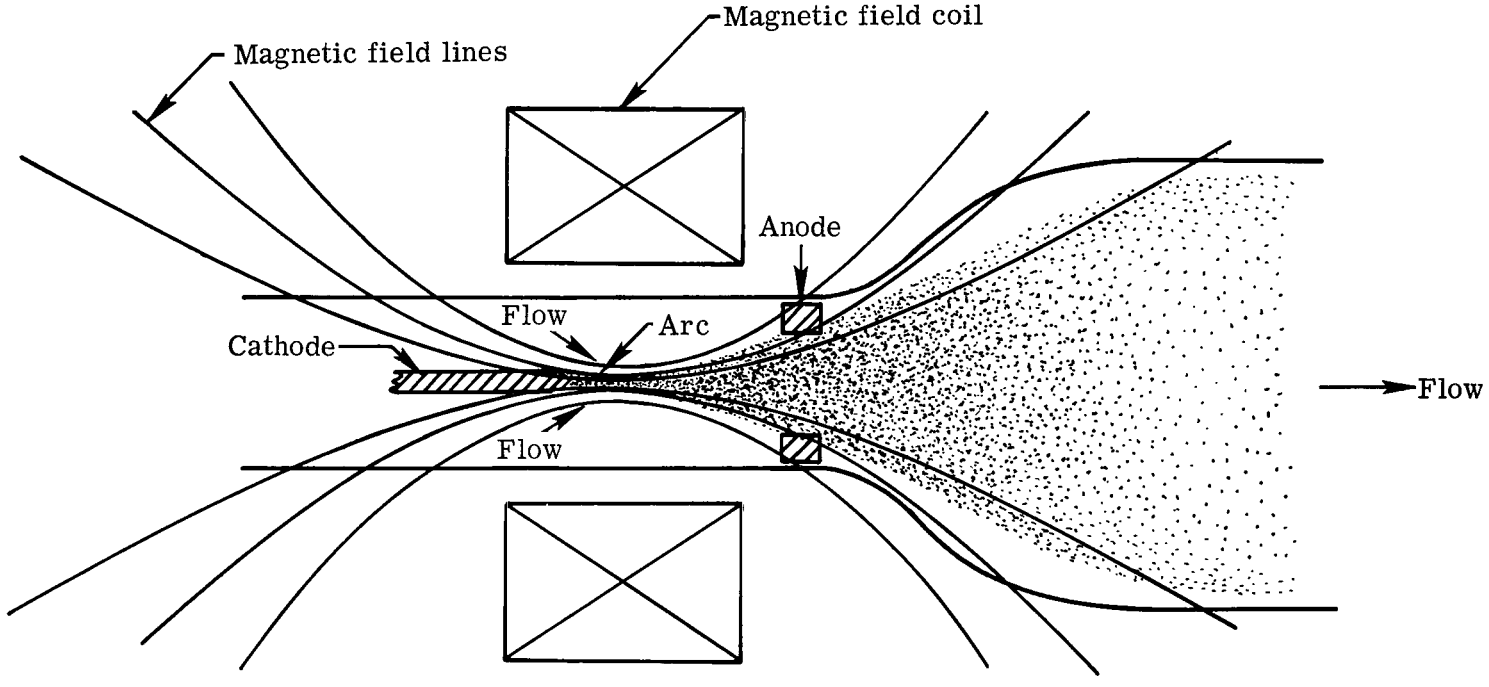

Figure 16.- Flow diagram of magnetic-nozzle device.

NATIONAL AERONAUTICS AND SPACE ADMINISTRATION
WASHINGTON, D. C. 20546

OFFICIAL BUSINESS

FIRST CLASS MAIL

POSTAGE AND FEES PAID
NATIONAL AERONAUTICS AND
SPACE ADMINISTRATION

POSTMASTER: If Undeliverable (Section 158 Postal Manual) Do Not Return

"The aeronautical and space activities of the United States shall be conducted so as to contribute . . . to the expansion of human knowledge of phenomena in the atmosphere and space. The Administration shall provide for the widest practicable and appropriate dissemination of information concerning its activities and the results thereof."

—NATIONAL AERONAUTICS AND SPACE ACT OF 1958

NASA SCIENTIFIC AND TECHNICAL PUBLICATIONS

TECHNICAL REPORTS: Scientific and technical information considered important, complete, and a lasting contribution to existing knowledge.

TECHNICAL NOTES: Information less broad in scope but nevertheless of importance as a contribution to existing knowledge.

TECHNICAL MEMORANDUMS: Information receiving limited distribution because of preliminary data, security classification, or other reasons.

CONTRACTOR REPORTS: Scientific and technical information generated under a NASA contract or grant and considered an important contribution to existing knowledge.

TECHNICAL TRANSLATIONS: Information published in a foreign language considered to merit NASA distribution in English.

SPECIAL PUBLICATIONS: Information derived from or of value to NASA activities. Publications include conference proceedings, monographs, data compilations, handbooks, sourcebooks, and special bibliographies.

TECHNOLOGY UTILIZATION PUBLICATIONS: Information on technology used by NASA that may be of particular interest in commercial and other non-aerospace applications. Publications include Tech Briefs, Technology Utilization Reports and Notes, and Technology Surveys.

Details on the availability of these publications may be obtained from:

SCIENTIFIC AND TECHNICAL INFORMATION DIVISION

NATIONAL AERONAUTICS AND SPACE ADMINISTRATION

Washington, D.C. 20546